

Simultaneous Attitude Control and Energy Storage using VSCMGs: Theory and Simulation

David J. Richie¹ and Panagiotis Tsiotras²

*School of Aerospace Engineering
Georgia Institute of Technology, Atlanta, GA, 30332-0150*

Jerry L. Fausz³

*Space Vehicle Component Technologies
Air Force Research Laboratory, Kirtland AFB, NM, 87117*

Abstract

This work examines the simultaneous use of single-gimbal Variable Speed Control Moment Gyroscopes (VSCMGs) as spacecraft attitude control actuators and energy storage devices. The resulting theory, initially developed in [5], is refined and simplified. The validity of the theory is demonstrated via numerical simulation.

1 Introduction

Space vehicle programs consistently seek to reduce satellite bus mass to increase payload capacity and/or reduce launch and fabrication costs. In addition, satellite system performance demands continually challenge space vehicle designers. Flywheel-based systems providing both energy storage and attitude control address the requirement of reducing the satellite bus mass by combining subsystem functionality. In particular, the Air Force Research Laboratory's (AFRL)'s Flywheel Attitude Control, Energy Transmission and Storage (FACETS) program will combine all, or part, of the energy storage, attitude control, and power management and distribution (PMAD) subsystems into a single system, significantly decreasing bus mass (and volume) [5].

An Integrated Power and Attitude Control System (IPACS) such as FACETS employs flywheels as "mechanical batteries" to perform the attitude control and energy storage functions. The IPACS concept eliminates vehicle mass while improving system performance and lifetime. Several attempts have been proposed in the past for developing an IPACS system. The use of flywheels instead of batteries to store energy on spacecraft was suggested by Roes [15] as early as 1961, when a 17 W hr/kg composite flywheel spinning at 10K to 20K RPM on magnetic bearings was proposed. The configuration included two counter-rotating flywheels, and the author did not mention the possibility of using the momentum for attitude control. This idea

grew over the next three decades. References [2, 3, 12] are representative of the period from 1970-1977, during which the term IPACS was coined [2] to describe an integrated power storage and attitude control system; this system was envisioned that could significantly reduce payload to orbit for shuttle-era satellite programs. Around that time NASA, in collaboration with the Draper Laboratory, completed various concept feasibility studies and even held several working groups in order to investigate potential implementation of IPACS [1, 4, 6, 14, 19]. Up until now, the well-documented IPACS concept has never been implemented due to high flywheel spin rates required for an IPACS system (on the order of 40K to 80K RPM versus less than 5K RPM for conventional Control Moment Gyroscopes (CMGs) or momentum wheel actuators). At such high speeds, the actuators quickly wear out mechanical bearings. Additional challenges include flywheel material mass/durability and stiffness inadequacies. Recently, the advent of advanced composite materials and magnetic bearing technology enables has enabled realistic IPACS development [5, 8, 18].

The control problem of simultaneous energy storage and attitude control is far from trivial, even in its simplest conceivable form. While decoupling the attitude control and energy storage functions may be a workable solution, research in related areas suggests it may not be the best approach [5]. It has been shown in [18] that simultaneous momentum management and power tracking can be accomplished with four or more wheels in momentum wheel (MW) mode. This is done by adjusting the wheel acceleration in the null subspace of the required attitude control torque dynamics matrix in such a way as to generate the required vehicle power while not imparting adverse external torque on the spacecraft. Furthermore, this method was shown to be practical for tracking the required attitude and power history profiles for several types of satellites and realistic on-orbit examples. [8, 18].

In this work, we revisit the problem of simultaneous attitude and power tracking for a rigid spacecraft using Variable Speed Control Moment Gyroscopes (VSCMGs). The derivation is based on an arbitrary number of VSCMGs and is independent of any particular VSCMG configuration. The use of VSCMGs instead of momentum wheels may be beneficial in cer-

¹Graduate Student, E-mail: gte979s@prism.gatech.edu, Tel: (404) 894-9108, Fax: (404) 894-2760

²Associate Professor, E-mail: p.tsiotras@ae.gatech.edu, Tel: (404) 894-9526, Fax: (404) 894-2760

³Research Engineer, E-mail: jerry.fausz@kirtland.af.mil, Tel:(505) 846-7890, Fax: (505)846-8977

tain applications that require large slew maneuvers. On the other hand, a MW-based IPACS system seems to be better suited for station-keeping applications. We derive the exact, nonlinear equation for the spacecraft/VSCMG system using minimal assumptions. The explicit derivation presented herein enables direct application of the theory to an actual satellite system. The generality of the theory permits application to a wide variety of spacecraft missions. This creates flexibility for future space systems contemplating an IPACS using VSCMGs for attitude control and energy storage.

2 Theoretical Developments

2.1 Notation

Matrices will be presented in bold as in \mathbf{A} , vectors will be presented with an arrow as in \vec{x} , and vector components with respect to a particular basis (essentially used as $n \times 1$ column matrices) will be denoted in italics as in x . The derivative of a vector \vec{x} with respect to the inertial reference frame will be denoted by

$$\frac{N d}{dt}(\vec{x}) \equiv \dot{\vec{x}}$$

For convenience, in representing vector cross products, we define the skew symmetric operator $\tilde{\mathbf{x}} \in \mathbb{R}^{3 \times 3}$, for $x \in \mathbb{R}^3$, which abbreviates the cross product between a vector x and a vector y as in $\vec{x} \times \vec{y} = \tilde{\mathbf{x}}y$ where $\tilde{\mathbf{x}}$ is given by

$$\tilde{\mathbf{x}} = \begin{bmatrix} 0 & -x_3 & x_2 \\ x_3 & 0 & -x_1 \\ -x_2 & x_1 & 0 \end{bmatrix}$$

The \otimes operator represents the Kronecker product of two matrices. For any two matrices $A \in \mathbb{R}^{n \times m}$ and $B \in \mathbb{R}^{p \times q}$ the matrix $A \otimes B$ is the $\mathbb{R}^{m \times n}$ matrix given by

$$A \otimes B = \begin{bmatrix} a_{11}B & a_{12}B & \cdots & a_{1n}B \\ a_{21}B & a_{22}B & \cdots & a_{2n}B \\ \vdots & \vdots & \ddots & \vdots \\ a_{m1}B & a_{m2}B & \cdots & a_{mn}B \end{bmatrix}$$

2.2 Assumptions and Definitions

We make several key assumptions throughout the derivation of the system model. These assumptions will be identified individually in the text as they become appropriate. For the development of the equations of motion, we consider a system consisting of a rigid spacecraft with body fixed reference frame, \mathcal{B} , which includes an array of n rigid VSCMGs with reference frames fixed to each of the VSCMG gimbals, $\mathcal{G}_1, \mathcal{G}_2, \dots, \mathcal{G}_n$. Figure 1 (taken from [17]) illustrates the \mathcal{G} frame for one VSCMG. As shown in Fig. 1, the frames attached to the n VSCMGs, \mathcal{G}_j , $j = 1, \dots, n$, are characterized by an orthogonal set of unit vectors, \hat{g}_{sj} , \hat{g}_{tj} , and \hat{g}_{gj} , $j = 1, \dots, n$, where the subscripts s , t , and g denote the spin, transverse and gimbal axes, respectively, satisfying the relation

$$\hat{g}_{gj} \times \hat{g}_{sj} = \hat{g}_{tj}, \quad j = 1, \dots, n$$

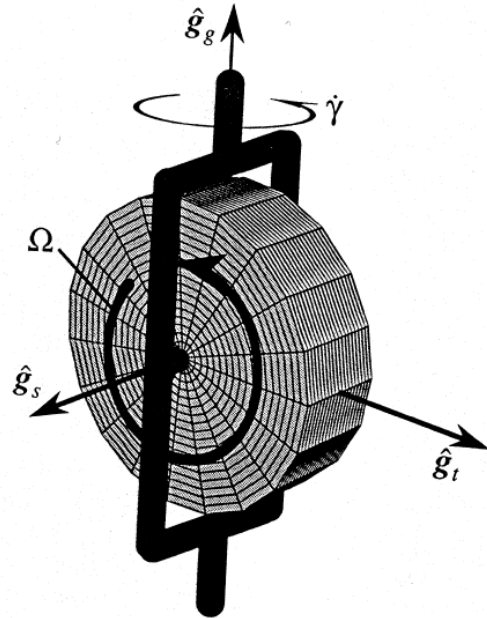


Figure 1: Variable Speed Control Moment Gyro (from [17]).

The matrix $\mathbf{L}_{BGj} \in \mathbb{R}^{3 \times 3}$ is the rotation matrix transforming vectors expressed as components in reference frame \mathcal{G}_j to frame \mathcal{B} and conversely, $\mathbf{L}_{GjB} = \mathbf{L}_{BGj}^T$ is the rotation matrix from \mathcal{B} to \mathcal{G}_j . Conveniently, the matrix $\mathbf{L}_{BGj} \in \mathbb{R}^{3 \times 3}$ can be defined as

$$\mathbf{L}_{BGj} = [\hat{g}_{sj} \ \hat{g}_{tj} \ \hat{g}_{gj}] \quad (1)$$

Next, let $\Omega \in \mathbb{R}^n$ be the column vector that contains the wheel rotational speeds of the n VSCMGs, Ω_j , $j = 1, \dots, n$, and let $\gamma \in \mathbb{R}^n$ be the column vector that contains the gimbal angles of the n VSCMGs, γ_j , $j = 1, \dots, n$. Then, $\dot{\Omega} \in \mathbb{R}^n$, $\dot{\gamma} \in \mathbb{R}^n$, and $\ddot{\gamma} \in \mathbb{R}^n$ are defined similarly.

To simplify the presentation of the results, we first define $\mathbf{G}_s \in \mathbb{R}^{3 \times n}$ as a matrix whose columns are the unit vectors of the n VSCMGs in the spin axis direction, so that

$$\mathbf{G}_s = [\hat{g}_{s1} \ \cdots \ \hat{g}_{sn}]$$

and we define \mathbf{G}_t and \mathbf{G}_g similarly for the transverse and gimbal axis unit vectors, respectively. We also define the matrix $\mathbf{G}_{sd} \in \mathbb{R}^{3 \times n}$ such that

$$\mathbf{G}_{sd} = \text{diag}\{\hat{g}_{s1}, \hat{g}_{s2}, \dots, \hat{g}_{sn}\}$$

and similarly for \mathbf{G}_{td} and \mathbf{G}_{gd} .

Next, it will be convenient to define several matrices involving the inertia properties of the VSCMGs. The inertia values of each VSCMG is decomposed into the contributions of the wheel and the gimbal structure using the scalar variables I_{Wsj} , I_{Wtj} , I_{Wgj} , I_{Gsj} , I_{Gtj} , and I_{Ggj} , $j = 1, \dots, n$, where the subscripts W and G denote the wheel and gimbal structure contributions

along the s , t , and g axes, respectively. We assume that all VSCMGs are perfectly balanced and aligned so that the unit vectors \hat{g}_{sj} , \hat{g}_{tj} , and \hat{g}_{gj} , $j = 1, \dots, n$, represent principle directions for the VSCMG reference frames.

Next, we define the inertia matrices

$$\begin{aligned} \mathbf{I}_{G_j} &= \text{diag}\{I_{G_{sj}}, I_{G_{tj}}, I_{G_{gj}}\} \\ \mathbf{I}_{G_s} &= [I_{G_{s1}} I_{G_{s2}} \cdots I_{G_{sn}}] \\ \mathbf{I}_{G_{sd}} &= \text{diag}\{\mathbf{I}_{G_s}\} \\ \mathbf{I}_{G_{sm}} &= \mathbf{I}_{G_{sd}} \otimes \mathbf{I}_3 \end{aligned} \quad (2)$$

where $\mathbf{I}_{G_j} \in \mathbb{R}^3$, $\mathbf{I}_{G_s} \in \mathbb{R}^{1 \times n}$, $\mathbf{I}_{G_{sd}} \in \mathbb{R}^{n \times n}$, and $\mathbf{I}_{G_{sm}} \in \mathbb{R}^{3n \times 3n}$. Similarly, we can define matrices for the other gimbal structure inertias: $\mathbf{I}_{G_t} \in \mathbb{R}^{1 \times n}$, $\mathbf{I}_{G_g} \in \mathbb{R}^{1 \times n}$, $\mathbf{I}_{G_{td}} \in \mathbb{R}^{n \times n}$, $\mathbf{I}_{G_{gd}} \in \mathbb{R}^{n \times n}$, $\mathbf{I}_{G_{tm}} \in \mathbb{R}^{n \times n}$, and $\mathbf{I}_{G_{gm}} \in \mathbb{R}^{n \times n}$; as well as for the wheel inertias: $\mathbf{I}_{W_j} \in \mathbb{R}^3$, $\mathbf{I}_{W_s} \in \mathbb{R}^{1 \times n}$, $\mathbf{I}_{W_t} \in \mathbb{R}^{1 \times n}$, $\mathbf{I}_{W_g} \in \mathbb{R}^{1 \times n}$, $\mathbf{I}_{W_{sd}} \in \mathbb{R}^{n \times n}$, $\mathbf{I}_{W_{td}} \in \mathbb{R}^{n \times n}$, $\mathbf{I}_{W_{gd}} \in \mathbb{R}^{n \times n}$, $\mathbf{I}_{W_{sm}} \in \mathbb{R}^{3n \times 3n}$, $\mathbf{I}_{W_{tm}} \in \mathbb{R}^{3n \times 3n}$, and $\mathbf{I}_{W_{gm}} \in \mathbb{R}^{3n \times 3n}$; and that \mathbf{I}_3 is the 3×3 identity matrix.

At times it is convenient to combine the inertia contributions of the wheel and gimbal structure, so we define $\mathbf{J}_j \in \mathbb{R}^{3 \times 3}$, $\mathbf{J}_s \in \mathbb{R}^{1 \times n}$, $\mathbf{J}_{sm} \in \mathbb{R}^{3n \times 3n}$, and $\mathbf{J}_{sb} \in \mathbb{R}^{3 \times 3n}$ such that

$$\begin{aligned} \mathbf{J}_j &= \mathbf{I}_{G_j} + \mathbf{I}_{W_j} \\ \mathbf{J}_s &= \mathbf{I}_{G_s} + \mathbf{I}_{W_s} \\ \mathbf{J}_{sm} &= \mathbf{I}_{G_{sm}} + \mathbf{I}_{W_{sm}} \\ \mathbf{J}_{sb} &= \mathbf{J}_s \otimes \mathbf{I}_3 \end{aligned}$$

and similarly for $\mathbf{J}_t \in \mathbb{R}^{1 \times n}$, $\mathbf{J}_g \in \mathbb{R}^{1 \times n}$, $\mathbf{J}_{tm} \in \mathbb{R}^{3n \times 3n}$, $\mathbf{J}_{gm} \in \mathbb{R}^{3n \times 3n}$, $\mathbf{J}_{tb} \in \mathbb{R}^{3 \times 3n}$, and $\mathbf{J}_{gb} \in \mathbb{R}^{3 \times 3n}$.

Finally, we define matrices $\boldsymbol{\Omega}_d \in \mathbb{R}^{n \times n}$ and $\boldsymbol{\omega}_d \in \mathbb{R}^{3n \times n}$ such that

$$\begin{aligned} \boldsymbol{\omega}_d &= \text{diag}\{\omega, \omega, \dots, \omega\} = \mathbf{I}_n \otimes \omega \quad (3) \\ \boldsymbol{\Omega}_d &= \text{diag}\{\Omega_1, \Omega_2, \dots, \Omega_n\} \quad (4) \end{aligned}$$

where the spacecraft body angular velocity vector $\omega \in \mathbb{R}^3$ is repeated n times in the definition of $\boldsymbol{\omega}_d$.

2.3 Dynamics

In this section we present the spacecraft dynamic system model extending the results of Oh and Vadali [13] to the case of VSCMGs. The equations of motion are derived using Euler's equation [11]

$$\dot{\boldsymbol{\tau}}^{\text{sys}/O} = \frac{N}{dt} \left(\vec{h}^{\text{sys}/O} \right) \quad (5)$$

where $\vec{h}^{\text{sys}/O}$ is the total angular momentum of the spacecraft and the VSCMG cluster about the combined system center of mass (point O), given by

$$\begin{aligned} \vec{h}^{\text{sys}/O} &= \vec{h}^{\text{P}/\text{P}^*} + \vec{h}^{\text{P}^*/O} + \vec{h}^{\text{W}/\text{W}^*} \\ &+ \vec{h}^{\text{W}^*/O} + \vec{h}^{\text{G}/\text{G}^*} + \vec{h}^{\text{G}^*/O} \end{aligned} \quad (6)$$

and $\vec{\tau}^{\text{sys}/O}$ is the sum of all external torques on the spacecraft expressed in \mathcal{B} . $\vec{h}^{\text{P}/\text{P}^*}$ is the angular momentum of the spacecraft bus (without the VSCMGs installed) about its own center of mass P^* . Similarly, $\vec{h}^{\text{G}/\text{G}^*}$ is the sum of the n -VSCMG gimbal structure angular momenta about each gimbal structure's center of mass, G_j^* , and $\vec{h}^{\text{W}/\text{W}^*}$ is the sum of n -VSCMG wheel angular momenta about each wheel's center of mass, W_j^* , respectively. For the remainder of this paper, we assume that the points G_j^* and W_j^* coincide for each VSCMG. Additionally, $\vec{h}^{\text{P}^*/O}$ is the angular momentum of the center of mass of the satellite bus (located at P^*) with respect to point O, $\vec{h}^{\text{W}^*/O}$ is the sum total of each wheel's center of mass angular momentum (located at point G_j^*) with respect to point O, and $\vec{h}^{\text{G}^*/O}$ is the sum total of each gimbal structure's center of mass angular momentum (located at point G_j^*) with respect to point O.

Let τ be $\vec{\tau}^{\text{sys}/O}$ expressed in \mathcal{B} . Then, the system dynamic equations of motion may be expressed as [13]

$$\tau = \mathbf{I}_T \dot{\omega} + \tilde{\omega} \mathbf{I}_T \omega + \mathbf{B} \ddot{\gamma} + \mathbf{D}_s \dot{\gamma} + \mathbf{E} \dot{\Omega} + \mathbf{F} \Omega \quad (7)$$

where ω is the angular velocity vector of the spacecraft body with respect to frame \mathcal{N} expressed in frame \mathcal{B} , τ is as defined above, and \mathbf{I}_T is the *total* inertia matrix given by

$$\mathbf{I}_T = \mathbf{I}_{sc} + \sum_{j=1}^N \mathbf{L}_{BG_j} \mathbf{J}_j \mathbf{L}_{BG_j}^T \quad (8)$$

where \mathbf{I}_{sc} is the spacecraft bus inertia about its own center of mass, P^* , plus the inertia of its center of mass about point O, and the total point mass inertias of the n -VSCMGs (i.e. the sum of each wheel's center of mass inertia about the total system center of mass, point O, as well as the sum of each gimbal structure's center of mass inertia about point O). This can be expressed as:

$$\mathbf{I}_{sc} = \mathbf{I}^{\text{P}/\text{P}^*} + \mathbf{I}^{\text{P}^*/O} + \mathbf{I}^{\text{G}^*/O} + \mathbf{I}^{\text{W}^*/O} \quad (9)$$

Note that the summation term in (8) is the time varying portion of the total inertia that changes as the VSCMGs move on the spacecraft. In addition, the coefficient matrices in (7) are given by

$$\mathbf{B} = \mathbf{G}_g (\mathbf{I}_{G_{gd}} + \mathbf{I}_{W_{gd}}) \quad (10)$$

$$\mathbf{D}_s(\omega, \Omega, \gamma) = \mathbf{D}_1 + \mathbf{D}_2 + \mathbf{D}_3 \quad (11)$$

$$\mathbf{E}(\gamma) = \mathbf{G}_s \mathbf{I}_{W_{sd}} \quad (12)$$

$$\mathbf{F}(\omega, \gamma) = \tilde{\omega} \mathbf{G}_s \mathbf{I}_{W_{sd}} \quad (13)$$

where

$$\begin{aligned} \mathbf{D}_1(\omega, \Omega, \gamma) &= \left(\mathbf{G}_t \mathbf{G}_{sd}^T \mathbf{I}_{W_{sm}} - \mathbf{G}_s \mathbf{G}_{td}^T \mathbf{I}_{W_{tm}} \right) \boldsymbol{\omega}_d \\ &+ \mathbf{G}_t \mathbf{I}_{W_{sd}} \boldsymbol{\Omega}_d \end{aligned} \quad (14)$$

$$\mathbf{D}_2(\omega) = \tilde{\omega} \mathbf{G}_g \mathbf{J}_{gd} \quad (15)$$

$$\begin{aligned} \mathbf{D}_3(\omega, \gamma) &= [(\mathbf{G}_t \mathbf{G}_{sd}^T \mathbf{I}_{G_{sm}} - \mathbf{G}_s \mathbf{G}_{td}^T \mathbf{I}_{G_{tm}}) \\ &- (\mathbf{G}_t \mathbf{G}_{sd}^T \mathbf{J}_{tm} - \mathbf{G}_s \mathbf{G}_{td}^T \mathbf{J}_{sm})] \boldsymbol{\omega}_d \end{aligned} \quad (16)$$

2.4 Kinematics

We represent the spacecraft orientation using the quaternion corresponding to the transformation from the inertial reference frame, \mathcal{N} , to the vehicle body frame, \mathcal{B} , as $\beta \triangleq [\beta_0 \ \beta_1 \ \beta_2 \ \beta_3]^T$. If we define the matrix $\mathbf{Q}(\beta)$ as

$$\mathbf{Q}(\beta) \triangleq \begin{bmatrix} -\beta_1 & -\beta_2 & -\beta_3 \\ \beta_0 & -\beta_3 & \beta_2 \\ \beta_3 & \beta_0 & -\beta_1 \\ -\beta_2 & \beta_1 & \beta_0 \end{bmatrix} \quad (17)$$

then the spacecraft's kinematic differential equation is:

$$\dot{\beta} \triangleq \frac{1}{2} \mathbf{Q}(\beta) \omega \quad (18)$$

Equations (7) and (18) together form the spacecraft's equations of motion.

2.5 Attitude Tracking

In this section we develop a control law for attitude tracking using VSCMGs. We begin by deriving a Lyapunov based steering control law as developed in [13] and then formulate the power tracking control in a somewhat analogous manner to that done for MWs in [8, 18].

To this end, we define a positive definite Lyapunov function in terms of the attitude errors $\beta_e = \beta - \beta_r$ and $\omega_e = \omega - \omega_r$ as follows

$$V = k(\beta - \beta_r)^T(\beta - \beta_r) + \frac{1}{2}(\omega - \omega_r)^T \mathbf{I}_T(\omega - \omega_r) \quad (19)$$

where β_r and ω_r are the desired vehicle reference attitude and reference angular velocity, respectively, and $k > 0$. The derivative of the Lyapunov function can be expressed as

$$\begin{aligned} \dot{V} &= -(\omega - \omega_r)^T \left[k\mathbf{Q}^T(\beta)\beta_r + \mathbf{I}_T\dot{\omega}_r - \mathbf{I}_T\dot{\omega} \right. \\ &\quad \left. - \frac{1}{2}\dot{\mathbf{I}}_T\omega + \frac{1}{2}\dot{\mathbf{I}}_T\omega_r \right] \end{aligned} \quad (20)$$

It is evident that \dot{V} can be made non-positive if we set

$$\begin{aligned} \mathbf{K}(\omega - \omega_r) &= \left[k\mathbf{Q}^T(\beta)\beta_r + \mathbf{I}_T\dot{\omega}_r - \mathbf{I}_T\dot{\omega} \right. \\ &\quad \left. + \frac{1}{2}\dot{\mathbf{I}}_T(\omega - \omega_r) \right] \end{aligned} \quad (21)$$

where \mathbf{K} is a positive definite gain matrix. Since \dot{V} is non-negative definite, the resulting system is Lyapunov stable. It can be shown that \dot{V} is zero if and only if $\omega = \omega_r$ and $\beta = \beta_r$. By LaSalle's theorem, one can show that the system trajectories are stabilized about the desired reference attitude. In addition, due to the radial unboundedness of V , the resulting system is actually globally asymptotically stable in the attitude and angular velocity error space.

Next, notice that the term $\frac{1}{2}\dot{\mathbf{I}}_T(\omega - \omega_r)$ is a linear function of $\dot{\gamma}$. Hence, we can decompose this term as follows

$$\mathbf{R}\dot{\gamma} = \frac{1}{2}\dot{\mathbf{I}}_T(\omega - \omega_r) \quad (22)$$

where the term \mathbf{R} is given by

$$\mathbf{R} = \frac{1}{2}(\mathbf{J}_{sb} - \mathbf{J}_{tb}) \left(\mathbf{G}_{sd}\mathbf{G}_{td}^T + \mathbf{G}_{td}\mathbf{G}_{sd}^T \right) (\omega_{rd} - \omega_d) \quad (23)$$

If we define a matrix \mathbf{D} such that $\mathbf{D} = \mathbf{D}_s + \mathbf{R}$ then we can combine (7), (20), (21), and (23) to yield the condition

$$\begin{aligned} \mathbf{B}\ddot{\gamma} + \mathbf{E}\dot{\Omega} + \mathbf{D}\dot{\gamma} + \mathbf{F}\Omega &= \\ \mathbf{K}(\omega - \omega_r) - k\mathbf{Q}^T(\beta)\beta_r - \mathbf{I}_T\dot{\omega}_r - \tilde{\omega}\mathbf{I}_T\omega + \tau_d \end{aligned} \quad (24)$$

where τ_d represents a disturbance torque on the vehicle.

2.6 Required Torque for Attitude Tracking

Next, we define the required torque vector $\tau_r \in \mathbb{R}^3$ as

$$\tau_r = \mathbf{K}(\omega - \omega_r) - k\mathbf{Q}^T(\beta)\beta_r - \mathbf{I}_T\dot{\omega}_r - \tilde{\omega}\mathbf{I}_T\omega \quad (25)$$

then (24) can be written as

$$\mathbf{B}\ddot{\gamma} + \mathbf{E}\dot{\Omega} + \mathbf{F}\Omega + \mathbf{D}\dot{\gamma} = \tau_r + \tau_d \quad (26)$$

which expresses the torque required for tracking in terms of the physical parameters (or states) of the system.

As usual, if we assume that the gimbal accelerations are small, then we can rearrange the required torque equation in terms of gimbal rate and wheel acceleration, which represents the parameters typically controlled by commercial CMGs and MWs, respectively. The resulting steering law (known as the velocity steering law) is thus

$$\mathbf{E}\dot{\Omega} + \mathbf{D}\dot{\gamma} = \tau_r - \mathbf{F}\Omega \quad (27)$$

2.7 Gimbal Acceleration Control

The main advantage of a single-gimbal CMG is its torque amplification property [10]. In order to take advantage of this property, we need to provide a velocity command $\dot{\gamma}$ to the CMG (and keep $\ddot{\gamma}$ small). In fact, most standard CMG actuators are controlled via gimbal rate and *not* gimbal acceleration. Solving for $\ddot{\gamma}$ directly from (26) will require large gimbal acceleration commands and hence, large gimbal motor torques. Alternatively, we can choose a velocity command $\dot{\gamma}$ from (27) and then implement this velocity steering law via an outer control loop that will keep the actual $\dot{\gamma}$ close to the desired gimbal rates. This yields the following equation for the gimbal acceleration command (assuming the desired gimbal acceleration, $\ddot{\gamma}_d$, is negligible):

$$\ddot{\gamma} = \lambda(\dot{\gamma}_d - \dot{\gamma}), \quad \lambda > 0 \quad (28)$$

2.8 Power Tracking

The kinetic energy T_j of the j th actuator is given by

$$T_{Wj} = \frac{1}{2} \Omega_j^2 I_{Wsj} \quad (29)$$

The total energy is just the sum of each of the individual actuator energies $T_W = \sum_{j=1}^N T_{Wj}$. Taking the first derivative of the energy yields the power generated by the wheels

$$P_W = \Omega^T \mathbf{I}_{Wsd} \dot{\Omega} \quad (30)$$

2.9 Simultaneous Attitude and Power Tracking

The available control inputs are the rate of change of the wheel speeds and the angular velocity of the gimbals (for the case of the gimbal velocity steering law). Hence,

$$\dot{\Omega} = u_{mw} \quad \text{and} \quad \dot{\gamma} = u_{cmg} \quad (31)$$

where $u_{mw} \in \mathbb{R}^n$ and $u_{cmg} \in \mathbb{R}^n$ are the control inputs in the ‘‘momentum wheel’’ and ‘‘CMG’’ modes, respectively. Let the combined control input $u = [u_{mw}^T \ u_{cmg}^T]^T$. Then after some algebraic manipulation we can write

$$\begin{bmatrix} \mathbf{C}_{11} & \mathbf{C}_{12} \\ \mathbf{C}_{21} & \mathbf{C}_{22} \end{bmatrix} u = \begin{bmatrix} F_{pv} \\ P_{fv} \end{bmatrix} \quad (32)$$

where $\mathbf{C}_{11} = \mathbf{E}$, $\mathbf{C}_{12} = \mathbf{D}$, $\mathbf{C}_{21} = \Omega^T \mathbf{I}_{W_{sd}}$ and $\mathbf{C}_{22} = 0_N$. Furthermore,

$$F_{pv} = \tau_r - \mathbf{F}\Omega \quad \text{and} \quad P_{fv} = P_W \quad (33)$$

where F_{pv} is as defined in (27) and P_{fv} is defined in (30).

Defining $\mathbf{C}_1 \equiv [\mathbf{C}_{11} \ \mathbf{C}_{12}]$ and $\mathbf{C}_2 \equiv [\mathbf{C}_{21} \ \mathbf{C}_{22}]$, the equation for F_{pv} from (32) can be written as

$$\mathbf{C}_1 u = F_{pv} \quad (34)$$

The general solution to (34) is given by

$$u = \mathbf{C}_1^\dagger F_{pv} + u_n \quad (35)$$

where the symbol \dagger denotes the suitable generalized inverse, and $\mathbf{C}_1 u_n = 0$ (i.e., u_n is in the null space of \mathbf{C}_1 , $\mathcal{N}(\mathbf{C}_1)$). Now we can substitute (35) into the equation for P_{fv} from (32) so that

$$\mathbf{C}_2 u = \mathbf{C}_2 (\mathbf{C}_1^\dagger F_{pv} + u_n) = P_{fv} \quad (36)$$

and

$$\mathbf{C}_2 u_n = P_m \quad (37)$$

where $P_m = P_{fv} - \mathbf{C}_2 \mathbf{C}_1^\dagger F_{pv}$. Since $u_n \in \mathcal{N}(\mathbf{C}_1)$, we can find a vector ν such that

$$u_n = \mathbf{P}_N \nu \quad (38)$$

where $\mathbf{P}_N = \mathbf{I}_n - \mathbf{C}_1^\dagger \mathbf{C}_1$ is the orthogonal projection onto $\mathcal{N}(\mathbf{C}_1)$. Then, from (37) and (38), and making use of the fact that \mathbf{P}_N is a projection matrix, we see that we can choose u_n such that

$$u_n = \mathbf{P}_N \mathbf{C}_2^T (\mathbf{C}_2 \mathbf{P}_N \mathbf{C}_2^T)^{-1} P_m \quad (39)$$

This completes the solution for u of (35) for combined attitude and power tracking.

In summary, given the reference attitude to track, β_r and ω_r , the required power P_W and the state of the system β, ω, Ω and γ , one calculates the required attitude tracking torque τ_r from (25) and the corresponding control inputs u_{mw} and u_{cmg} from (35) and (39). If a gimbal acceleration steering law is required (to command the gimbal motors), then equation (28) must be used to ‘‘back-step’’ the velocity command $u_{cmg} = \dot{\gamma}_d$ to an acceleration command. Interestingly, the formulated power equation does not change regardless of these steering laws as $\dot{\gamma}$ and $\ddot{\gamma}$ do not appear in the power equation.

Table 1: Simulation Parameters

Symbol	Value	Units
N	4	unitless
θ	54.75	deg
$\omega(0)$	[0 0 0]	rad/sec
$\beta(0)$	[0.5 0.5 0.5 0.5]	unitless
$\gamma(0)$	$[\frac{\pi}{4} \ -\frac{\pi}{4} \ \frac{\pi}{4} \ \frac{\pi}{4}]$	rad
$\dot{\gamma}(0)$	[0 0 0 0]	rad
$\Omega(0)$	[15000 13000 7000 5000]	rpm
W_{sj0}	40	unitless
W_{gj0}	1	unitless
\mathbf{I}_{Wj}	diag{0.70, 0.20, 0.20}	Kg m ²
\mathbf{I}_{Gj}	diag{0.10 0.10 ,0.10}	Kg m ²
\mathbf{I}_{sc}	diag{15053, 6510, 11122}	Kg m ²
\mathbf{K}	diag{700, 700, 700}	Kg m ² /sec
k	35	Kg m ² /sec
μ	1e-4	unitless
λ	1	unitless

3 Numerical Simulation

Next, we use a numerical simulation to demonstrate the validity of the control algorithm presented in the previous section. Similarly to references [13, 17], we use a standard four VSCMG pyramid configuration. In this configuration the VSCMGs are installed so that the four gimbal axes form a pyramid with respect to the body. The pyramid configuration has been implemented here in order to facilitate comparisons with the related literature even though the theory applies generically to the n actuator case. Table 1 contains the parameters used for the simulation. These parameters closely parallel those used in [13], [16], and [17]. The reference tracking maneuver is the one described in [18].

In Table 1 the parameter θ represents the pyramid angle of each VSCMG that is measured from the vehicle’s $b_1 - b_2$ plane to the VSCMG’s gimbal axis. The weighted generalized inverse \mathbf{C}_1^\dagger used in this work is given as [17]

$$\mathbf{C}_1^\dagger = \mathbf{W} \mathbf{C}_1^T (\mathbf{C}_1 \mathbf{W} \mathbf{C}_1^T)^{-1} \quad (40)$$

where \mathbf{W} is a diagonal MW/CMG mode weighting matrix $\mathbf{W} = \text{diag}\{\mathbf{W}_s, \mathbf{W}_g\}$, where \mathbf{W}_s and \mathbf{W}_g are the momentum wheel and CMG weighting matrices, respectively, given by $\mathbf{W}_s = \text{diag}\{W_{s1}, W_{s2}, W_{s3}, W_{s4}\}$ and similarly for \mathbf{W}_g . The matrix \mathbf{W}_g represents the weights for the CMG mode (to capitalize on the torque amplification property) and is chosen to be constant throughout a maneuver. The weight matrix \mathbf{W}_s is the MW mode matrix that comes into play near a CMG singularity. The elements of \mathbf{W}_s are given by

$$W_{sj} = W_{sj0} \exp^{-\mu\delta}, \quad j = 1, \dots, 4 \quad (41)$$

where the constant parameters μ and W_{sj0} are chosen by the control system designer to obtain the desired performance. The variable δ describes the proximity to a CMG singularity [7, 13, 16, 17]¹. The expression for δ used here is different than in [17] and is defined as the minimum singular value of \mathbf{C}_1 . This is a more accurate way to describe the singularity of the matrix \mathbf{C}_1 [9].

In the numerical simulation, the goal is to track a reference attitude and power profile. The given reference attitude trajectory used in this numerical example corresponds to a near-polar orbital satellite that has to meet specific sun and ground tracking requirements. It is similar to the example used in [18].

Figure 2 contains a plot of the vehicle attitude error time history. Figure 3 contains the vehicle angular velocity error time history. Figure 4 shows the actual and commanded power time histories. In this figure, two lines are shown but one is on top of the other, indicating very accurate tracking of the desired power profile. Furthermore, Figs. 5 and 6 show the VSCMG gimbal angle and wheel spin-rate time histories, respectively.

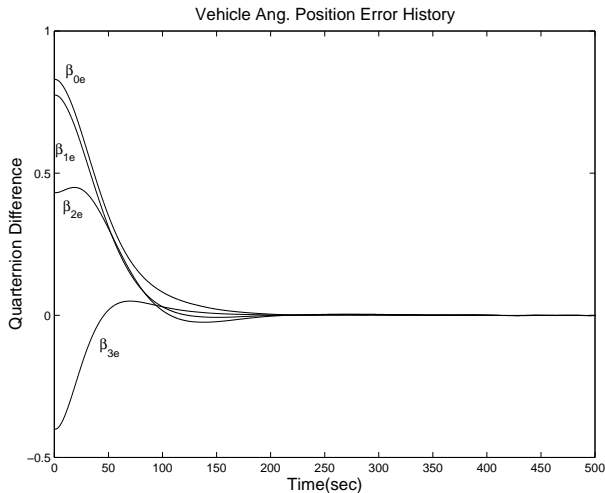


Figure 2: Vehicle Attitude Error Time History.

These results show that the vehicle attitude tracks the desired attitude. At the same time, the power profile is followed while not affecting the vehicle attitude, as desired.

4 Conclusions

In this paper we have developed a methodology for combined attitude control and energy storage using VSCMGs. The resulting control scheme simultaneously provides attitude control torque and energy storage torque while not imparting adverse torques on the satellite. Furthermore, we have investigated this methodology through numerical simulations. Future work will implement this control methodology on a

¹The CMG singularity is defined as a configuration where the matrix \mathbf{C}_1 is not full row rank.

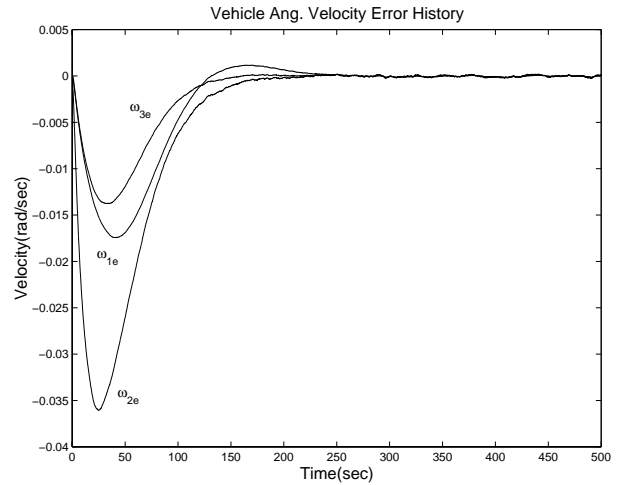


Figure 3: Vehicle Angular Velocity Error Time History.

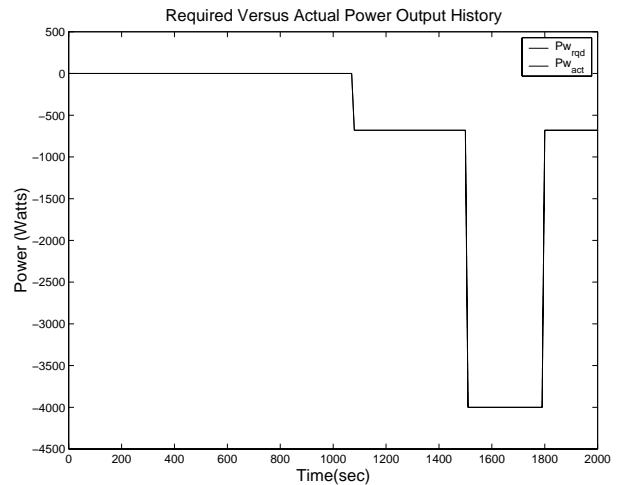


Figure 4: Actual and Commanded Power Profile.

more realistic space vehicle simulation model to be used for controller design, hardware-in-the-loop testing, and vehicle plant modeling. This will allow low cost attitude control and energy storage system design prior to implementing it on a real satellite. Finally, the culmination of this work will be a ground demonstration of flywheel hardware on a 3 degree-of-freedom spacecraft simulator at AFRL to validate combined attitude control and energy storage functionality.

Acknowledgement: The authors would like to thank Dr. Marc Jacobs of AFOSR for his support of this work via AFOSR grant F49620-00-1-0374. Part of this work was carried out during the visit of the first author to the AFRL/VS Directorate through the Educational Partnership Agreement between AFRL and the Georgia Institute of Technology (Contract no: 2000-AFRL/VS-EPA-15). Also, the authors are greatly indebted to H. Yoon for his help validating the simulation software.

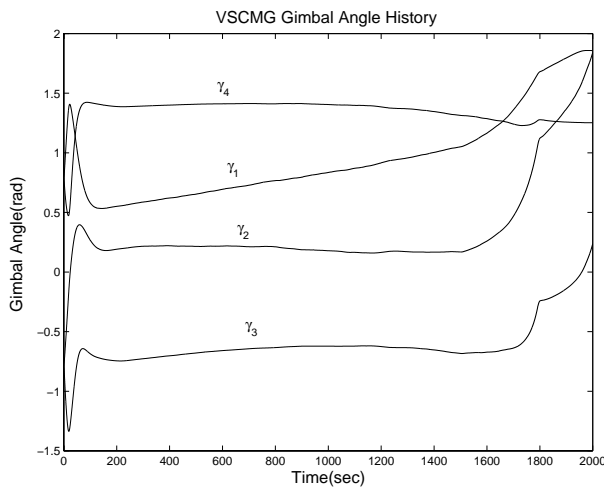


Figure 5: VSCMG Gimbal Angle History.

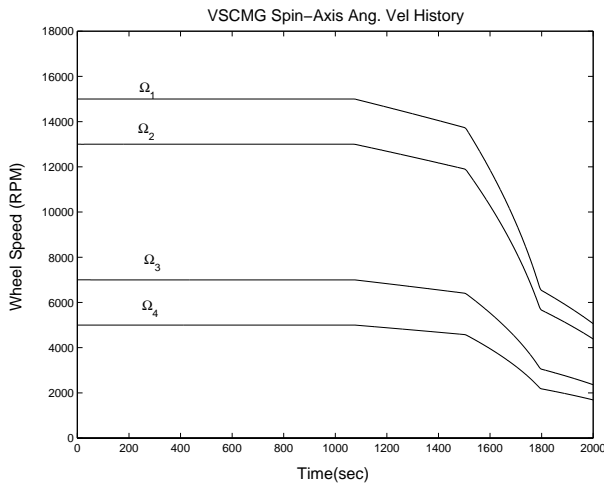


Figure 6: VSCMG Spin Rate History.

References

[1] D. Anand, J. A. Kirk, R. B. Amood, P. A. Studer, and G. E. Rodriguez, "System Considerations for Magnetically Suspended Flywheel systems," in *Proceedings of the 21st Intersociety Energy Conversion Engineering Conference*, vol. 3, pp. 1829–1833, 1986.

[2] W. W. Anderson and C. R. Keckler, "An Integrated Power/Attitude Control System (IPACS) for Space Application," in *Proceedings of the 5th IFAC Symposium on Automatic Control in Space*, 1973.

[3] A. Cormack III, "Three Axis Flywheel Energy and Control Systems," NASA Technical Report TN-73-G&C-8, North American Rockwell Corp., 1973.

[4] J. Downer, D. Eisenhaure, R. Hockney, B. Johnson, and S. O'Dea, "Magnetic Suspension Design Options for Satellite Attitude Control and Energy Storage," in *Proceedings of the 20th Intersociety Energy Conversion Engineering Conference*, vol. 2, pp. 424–430, 1985.

[5] J. Fausz and D. Richie, "Flywheel Simultaneous Attitude Control and Energy Storage using VSCMGs," in *IEEE International Conference on Control Applications*, pp. 991–995, Sept. 25–27 2000. Anchorage, AK.

[6] T. Flatley, "Tetrahedron Array of Reaction Wheels for Attitude Control and Energy Storage," *Proceedings of the 20th Intersociety Energy Conversion Engineering Conference*, Vol. 2, pp. 2353–2360, 1985.

[7] K. A. Ford and C. D. Hall, "Singular Direction Avoidance Steering for Control-Moment Gyros," *AIAA Journal of Guidance, Control, and Dynamics*, Vol. 23, No. 4, pp. 648–656, 2000.

[8] C. Hall, "High-Speed Flywheels for Integrated Energy Storage and Attitude Control," in *Proceedings of the American Control Conference*, pp. 1894–1898, June 4–6 1997. Albuquerque, NM.

[9] R. Horn and C. R. Johnson, *Matrix Analysis*, Cambridge, United Kingdom: Cambridge University Press, 1985.

[10] A. D. Jacot and D. Liska, "Control Moment Gyros in Attitude Control," *Journal of Spacecraft and Rockets*, Vol. 3, No. 9, pp. 1313–1320, 1966.

[11] T. Kane and D. Levinson, *Dynamics: Theory and Applications*, New York: McGraw-Hill, 1985.

[12] J. E. Notti, A. Cormack III, W. C. Schmill, and W. J. Klein, "Integrated Power/Attitude Control System (IPACS) Study: Volume II—Conceptual Designs," NASA Technical Report CR-2384, Rockwell International Space Division, Downey, CA, 1974.

[13] H. S. Oh and S. R. Vadali, "Feedback Control and Steering Laws for Spacecraft Using Single Gimbal Control Moment Gyros," *Journal of the Astronautical Sciences*, Vol. 39, No. 2, pp. 183–203, 1994.

[14] G. E. Rodriguez, P. A. Studer, and D. A. Baer, "Assessment of Flywheel Energy Storage for Spacecraft Power Systems," NASA Technical Memorandum TM-85061, NASA Goddard Space Flight Center, Greenbelt, MD, 1983.

[15] J. B. Roes, "An Electro-Mechanical Energy Storage System for Space Application," in *Progress in Astronautics and Rocketry*, vol. 3, (New York), pp. 613–622, Academic Press, 1961.

[16] H. Schaub and J. L. Junkins, "Singularity Avoidance Using Null Motion and Variable-Speed Control Moment Gyros," *AIAA Journal of Guidance, Control, and Dynamics*, Vol. 23, No. 1, pp. 11–16, 2000.

[17] H. Schaub, S. R. Vadali, and J. L. Junkins, "Feedback Control Law for Variable Speed Control Moment Gyros," *Journal of the Astronautical Sciences*, Vol. 46, No. 3, pp. 307–28, 1998.

[18] P. Tsiotras, H. Shen, and C. Hall, "Satellite Attitude Control and Power Tracking with Energy/Momentum Wheels," *AIAA Journal of Guidance, Control, and Dynamics*, Vol. 24, No. 1, pp. 23–34, 2001.

[19] K. E. Van Tassel and W. E. Simon, "Inertial Energy Storage for Advanced Space Station Application," in *Proceedings of the 20th Intersociety Energy Conversion Engineering Conference*, vol. 2, pp. 337–342, 1985.